第 24 卷第 11 期
2008 年 11 月

无 机 化 学 学 报
CHINESE JOURNAL OF INORGANIC CHEMISTRY

Vol.24 No.11
1794~1802

两种有机磺酸配合物的合成、表征及与 DNA 键合性质

李明田[1,2] 黄 俊[1] 周 璇[1] 王成刚*[,2]

([1]武汉理工大学光纤传感技术与信息处理教育部重点实验室,武汉 430070)

([2]华中师范大学化学学院,武汉 420079)

摘要:合成了 2 个新型有机磺酸配合物,$[Cd(phen)_2(ans)_2]\cdot H_2O$ (**1**)和$[Pb(phen)_2(ans)_2]\cdot H_2O$ (**2**) (phen=1,10-邻菲咯啉,ans=4-氨基-1-萘磺酸根),通过元素分析、红外光谱等对配合物进了表征,用 X-射线单晶衍射方法测定了配合物的单晶结构。应用紫外-可见吸收光谱、荧光光谱及粘度测定方法研究了配合物与 ctDNA 的作用,发现 2 个配合物均以插入和氢键两种模式与 ctDNA 发生作用。

关键词:有机磺酸配合物;晶体结构;ctDNA

中图分类号:O614.24+2;O614.53+1 **文献标识码**:A **文章编号**:1001-4861(2008)11-1794-09

Syntheses, Characterization, Crystal Structures and DNA-binding Properties of Two Complexes Containing Organosulfonate Ligand

LI Ming-Tian[1,2] HUANG Jun[1] ZHOU Xuan[1] WANG Cheng-Gang[2]

([1]*Key Laboratory of Fiber Optic Sensing Technology and Information Processing* (*Ministry of Education*), *Wuhan University of Technology, Wuhan* 430070)

([2]*College of Chemistry, Central China Normal University, Wuhan* 430079)

Abstract: Two organosulfonate complexes, $[M(phen)_2(ans)_2]\cdot H_2O$ (M=Cd **1**, M=Pb **2**), were obtained from the reaction of 1,10-phenanthroline (phen), sodium 4-aminonaphthalene-1-sulfonate tetrahydrate (Naans) and $Cd(OAc)_2\cdot 2H_2O$ or $Pb(NO_3)_2$ in a mixed solvent of water and methanol at 25 ℃. The compounds were characterized by elemental analysis, IR, and X-ray diffraction single crystal structure analyses. Interactions of the complexes with calf thymus DNA (ctDNA) were investigated by UV-Vis spectra, luminescence spectra (including luminescence titrations, steady-state emission quenching by $[Fe(CN)_6]^{4-}$, DNA competitive binding with ethidium bromide (EB)), and viscosity measurements. The experimental results indicated that there were two interactions between the complexes and DNA, namely the electrostatic interaction and intercalation, with the binding constants of 1.82×10^5 L·mol^{-1} for **1** and 4.96×10^4 L·mol^{-1} for **2** in buffer of 50 mmol·L^{-1} NaCl and 5 mmol·L^{-1} Tris-HCl (pH 7.0). CCDC: 669692, **1**; 674923, **2**.

Key words: organosulfonate complexes; crystal structures; ctDNA

The properties of DNA binding to transition-metal complex, especially polypyridyl Ru(Ⅱ) complexes, have been well studied[1~4]. It is found that the complex can bind to DNA in noncovalent binding fashions of electrostatic, groove, and intercalative binding including classical intercalation, semi-intercalation, and quasi-intercalation[4]. As far as the mixed-ligand complex is concerned, the planarity of its main ligand is thought to play a key role in interaction with DNA[5,6], and the ancillary ligand can make something indirectly affect on the DNA binding properties by changing the planarity of the main ligand and hydrophobicity of the

收稿日期:2008-04-28。收修改稿日期:2008-08-04。

国家自然科学基金资助重点项目(No.60537050)。

*通讯联系人。E-mail:wangcg23@yahoo.com.cn

第一作者:李明田,男,29 岁,博士研究生;研究方向:光电子及信息材料。

complex[7,8]. Due to the characteristic helical structure of DNA, the nucleic bases are located in an almost coplanar arrangement, which allows planar polycylic aromatic molecules to intercalate between two base pairs [9]. As far as we know, almost all intercalators are the cations of ogranometallic complex except for some organic dyes. In order to study further the DNA-binding mode of the complex, a series of mixed-ligand complexes constructed by aromatic sulfonate and bidentate chelating ligands such as 1,10-phenanthroline and 2,2′-bipyridine, were synthesized. These compounds were found exhibiting stronger fluorescence property in aqueous solution.

Herein, we prepared two new complexes, $[Cd(phen)_2(ans)_2]\cdot H_2O$ **1** and $[Pb(phen)_2(ans)_2]\cdot H_2O$ **2**, whose crystal structures were determined by single crystal X-ray diffraction. Both complexes also behave as the neutral complex because they were hardly ionized in aqueous solution, as proved by the conductivity. The DNA-binding properties of the complexes were explored by electronic absorption, fluorescence studies and viscosity measurements. Experimental results indicated that both complexes bind to DNA by means of two interactions of electrostatic interaction and intercalation modes.

1 Experimental

1.1 Preparation of complexes $[Cd(phen)_2(ans)_2]\cdot H_2O$ (1) and $[Pb(phen)_2(ans)_2]\cdot H_2O$ (2)

5.0 mL methanol solution of phenanthroline monohydrate (0.200 g, 1 mmol) was added to an aqueous solution (15 mL) of $Cd(OAc)_2\cdot 2H_2O$ (0.267 g, 1 mmol). After the mixture was stirred for about 2 h at 25 ℃, the solution was treated with sodium 4-aminonaphthalene-1-sulfonate tetrahydrate (0.642 g, 2 mmol) in 5 mL methanol. After filtration, the pale yellow solution was allowed to stand at room temperature. Crystals suitable for X-ray single crystal analysis were obtained by slow evaporation of solvent at room temperature (0.561 g, 60%). Calcd. for $C_{44}H_{34}CdN_6O_7S_2$ (%): C 56.51, H 3.68, N 8.97. Found (%): C 56.34, H 3.77, N 9.12%. IR (KBr disc, cm^{-1}): 3 450s, 3 360s, 3 247m, 3 064 w, 1 624m, 1 579m, 1 516s, 1 429m, 1 224m, 1 158s, 1 142s, 1 040s, 1 021m, 852w, 727s, 685s, 599m, 505w.

Complex **2** was prepared via analogous procedure to that used for **1** above, and $Pb(NO_3)_2$ (0.331 g, 1 mmol) replacing $Cd(OAc)_2\cdot 2H_2O$. Calcd. for $C_{44}H_{34}N_6O_7PbS_2$ (%): C 56.45, H 3.64, N 8.95. Found (%): C 56.11, H 3.84, N 8.87. IR (KBr pellet, cm^{-1}): 3 365s, 3 354m, 3 241 m, 3 066w, 1 627m, 1 571m, 1 515s, 1 425m, 1 214s, 1 177s, 1 143s, 1 036s, 1 016s, 842m, 722s, 680s, 596m. The molar conductances (Λ_m) in DMF are 16.8 and 17.5 $S\cdot cm^2\cdot mol^{-1}$ for **1** and **2**, respectively, indicating that two complexes are nonelectrolyte[10].

1.2 Physical measurements

Elemental analyses were performed on a Carlo Erba 1105 elemental analyzer. Infrared spectra (KBr disc, 4 000~400 cm^{-1}) were recorded on a FTIR NEXUS instrument. The pH of buffer solution was measured by DELTA pH instrument. UV-Visible spectra were carried out on UV-2450 spectrophotometer. Emission spectra were obtained on F-4500 fluorescence spectrophotometer. The conductivity was tested by JENCO Model 3010 conductivity meter.

All the experiments involving in the interaction of the complexes with DNA were carried out in aerated buffer (50 $mmol\cdot L^{-1}$ NaCl and 5 $mmol\cdot L^{-1}$ Tris-HCl, pH 7.0). The absorption and emission titrations with ctDNA were performed by keeping the concentrations of the complex constant while varying the DNA concentrations. A solution of ctDNA gave a ratio of UV absorbance at 260 and 280 nm of about 1.85∶1, indicating that the DNA was sufficiently free of protein. The concentration of DNA was calculated by ε_{260}=6 600 $L\cdot mol^{-1}\cdot cm^{-1}$ [11]. Steady-state emission quenching experiments were carried out using $[Fe(CN)_6]^{4-}$ as the quencher. The experiments of DNA competitive binding with EB were carried out in the buffer solution after DNA was pretreated with EB in the ratio c_{DNA}/c_{EB}=5 for 30 min, varying the concentrations of the complex at room temperature. Viscosity experiments were carried out on an Ubbelodhe viscometer immersed in a thermostated waterbath maintained at 28 ±0.1 ℃. Flow time was measured, and each sample was measured at least three times, and an average flow time calculated. Data were presented as $(\eta/\eta_0)^{1/3}$ vs c_M/c_{DNA}, where η and η_0 are the

viscosities of DNA in the presence and absence of the complex, respectively. Viscosity values were calculated from the observed flow time of DNA-containing solution (t>100 s) corrected for the flow time of buffer alone (t_0), $\eta=(t-t_0)/t_0$[12].

1.3 Crystal structure determination

X-ray diffraction data for the two complexes were collected on a Bruker SMART APEX CCD diffractometer with a graphite-monochromatized Mo $K\alpha$ radiation (λ=0.071 073 nm) at 19(2) ℃. A total of 12 089 and 24 255 reflections were collected in the range 1.73°~26.25° and 1.70°~27.50° using an ω scan mode for complexes **1** and **2**, respectively, of which 7 628 and 8 888 were unique (R_{int}=0.040 6 and 0.079 2) and 3 726 and 5 434 with $I>2\sigma(I)$ were considered as observed. An empirical absorption correction (SADABS) was applied to the raw intensities [13]. The structures were solved by direct methods and refined on F^2 by full-matrix least-squares techniques with SHELX-97 program[14]. All non-hydrogen atoms and hydrogen atoms were refined anisotropically and isotropically, respectively. Geometrical calculations and the molecular diagrams were obtained with the program PLATON[15]. The refinements were converged at R=0.035 6 and wR=0.085 3 ($w=1/[\delta^2(F_o^2)+(0.050\,0P)^2+0.131\,6P]$, $P=(F_o^2+2F_c^2)/3$, S=1.035, $(\Delta/\sigma)_{max}$=0.005) for **1** and R=0.063 2 and wR=0.112 2 ($w=1/[\delta^2(F_o^2)+(0.034\,0P)^2+5.353\,9P]$, $P=(F_o^2+2F_c^2)/3$, S=1.027, $(\Delta/\sigma)_{max}$=0.001) for **2**. The largest and minimum peaks in the final difference Fourier map were 500 and −422 e·nm^{-3} for **1** and 882 and −756 e·nm^{-3} for **2**, respectively. Crystal parameters and details of the data collection and structure refinement were given in Table 1. Selected bond lengths and angles were listed in Table 2. Because of the disorder about the ans ligand containing S1, the bond lengths and angles involving in the disorder atoms and Pb(Ⅱ) atom didn′t be listed in the table. The disordered atoms were refined using FVAR, second variable facility of SHELX-97 program.

CCDC: 669692, **1**; 674923, **2**.

Table 1 Crystallographic data for the complexes $[Cd(phen)_2(ans)_2]\cdot H_2O$ (1) and $[Pb(phen)_2(ans)_2]\cdot H_2O$ (2)

Crystal data	**1**	**2**
Empirical formula	$C_{44}H_{34}CdN_6O_7S_2$	$C_{44}H_{34}N_6O_7PbS_2$
Formula weight	935.29	1030.08
Crystal system	Triclinic	Monoclinic
Space group	$P\bar{1}$	$P2_1/n$
a / nm	1.247 56(8)	1.348 50(9)
b / nm	1.317 34(9)	1.602 13(11)
c / nm	1.363 40(9)	1.810 82(12)
α / (°)	98.514 0(10)	90
β / (°)	105.791 0(10)	95.453 0(10)
γ / (°)	111.664 0(10)	90
V / nm^3	1.924 9(2)	3.894 5(5)
Z	2	4
μ / mm^{-1}	0.739	4.502
F(000)	952	2 040
θ range for data collection / (°)	1.73~26.25	1.70~27.50
Index ranges	$-15\leqslant h\leqslant 10, -15\leqslant k\leqslant 16, -16\leqslant l\leqslant 16$	$-14\leqslant h\leqslant 17, -20\leqslant k\leqslant 20, -23\leqslant l\leqslant 14$
No. refln. /unique (R_{int})	12 089 / 7 628 (0.040 6)	24 255 / 8 888 (0.079 2)
Data / restraints / parameters	7 628 / 6 / 559	8 888 / 461 / 548
Goodness-of-fit on F^2	1.035	1.027
Final R indices [$I>2\sigma(I)$]	R_1=0.035 6, wR_2=0.085 3	R_1=0.063 2, wR_2=0.112 2
R indices (all data)	R_1=0.043 6, wR_2=0.090 8	R_1=0.115 4, wR_2=0.129 4
Largest difference peak and hole / (e·nm^{-3})	500 and −422	882 and −756

Table 2　Selected bond lengths (nm) and angles (°) for the complexes $[Cd(phen)_2(ans)_2]\cdot H_2O$ (1) and $[Pb(phen)_2(ans)_2]\cdot H_2O$ (2)

			1		
Cd(1)-O(1)	0.227 8(19)	Cd(1)-N(1)	0.236 6(2)	Cd(1)-N(3)	0.234 3(2)
Cd(1)-O(4)	0.227 0(2)	Cd(1)-N(2)	0.234 2(2)	Cd(1)-N(4)	0.263(2)
O(4)-Cd(1)-O(1)	88.13(8)	N(2)-Cd(1)-N(4)	89.96(7)	N(2)-Cd(1)-N(3)	107.66(7)
O(1)-Cd(1)-N(2)	152.09(7)	O(4)-Cd(1)-N(1)	106.91(8)	O(1)-Cd(1)-N(4)	100.32(7)
O(1)-Cd(1)-N(3)	100.23(7)	O(4)-Cd(1)-N(2)	92.55(7)	N(3)-Cd(1)-N(4)	70.86(7)
O(4)-Cd(1)-N(4)	156.63(8)	O(4)-Cd(1)-N(3)	86.28(7)	O(1)-Cd(1)-N(1)	81.85(7)
			2		
Pb(1)-N(2)	0.255 8(6)	Pb(1)-N(4)	0.254 4(7)	Pb(1)-O(3)	0.268 6(5)
Pb(1)-N(3)	0.255 9(6)	Pb(1)-N(5)	0.251 9(6)		
N(5)-Pb(1)-N(2)	84.8(2)	N(3)-Pb(1)-O(3)	76.13(17)	O(2B)-Pb(1)-O(3)	132.1(7)
N(4)-Pb(1)-N(2)	137.0(2)	N(5)-Pb(1)-N(4)	65.2(2)	N(4)-Pb(1)-N(3)	79.4(2)
N(5)-Pb(1)-O(3)	142.15(18)	N(2)-Pb(1)-O(3)	109.67(18)		
N(5)-Pb(1)-N(3)	79.45(18)	N(4)-Pb(1)-O(3)	82.11(18)		

2　Results and discussion

2.1　Crystal structure

In spite of the different cell systems, the asymmetric units of both complexes are identical, namely one neutral compound and one crystal water molecule. Thus, the crystal description is put emphasis on complex **1**. As shown in Fig.1, the Cd(Ⅱ) atom has a distorted octahedral environment, and is coordinated by four N atoms from two phen ligands and by two O atoms belonging to two monodentate ligands of ans. The distances of the Cd-N (Table 2), and the mean Cd-N is 0.235 35 (2) nm, which are shorter than the distances of Cd-N within $[(phen)_2Cd(\mu\text{-}SC_6H_4CH_3\text{-}p)]_2(PF_6)_2$ (0.236 5(4)~0.243 2(4) nm)[16], and longer than the length of the equivalent part in $[Cd_2(bipy)_4(H_2O)_2(1,5nds)](1,5nds)\cdot 4H_2O$ (0.232 8(3)~0.233 7(3) nm; bipy is 2.2′-bipyridine and 1,5nds is 1,5-naphthalenedisulfonate)[17]. The distances of Cd-O are 0.227 0(2) and 0.227 81(2) nm, which is in agreement with the Cd-O(S) distance in $[Cd(bipy)_2(H_2O)(peds)]\cdot 4H_2O$ (0.227 9(3) nm; peds is 4,4-phenyletherdisulfonate) and shorter than the Cd-O(S) distance of $[Cd_2(bipy)_4(H_2O)_2(1,5nds)](1,5nds)\cdot 4H_2O$ (0.232 0(2) nm)[17].

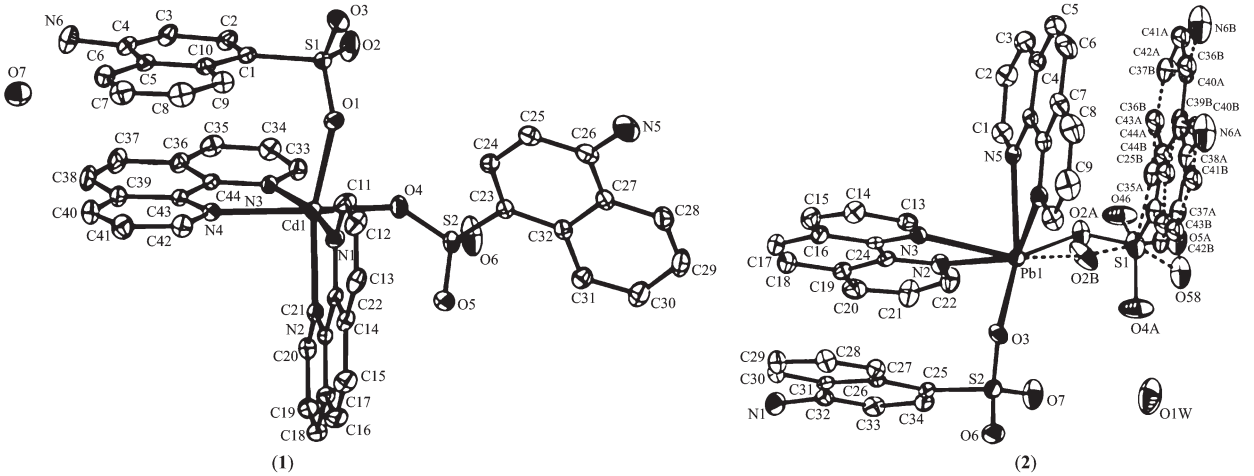

Disorder refining to a 0.646:0.354 ratio; H atoms are omitted for the clarity

Fig.1　ORTEP drawings with atomic numbering scheme at 30% for $[Cd(phen)_2(ans)_2]\cdot H_2O$ (**1**) and $[Pb(phen)_2(ans)_2]\cdot H_2O$ (**2**)

The phen rings are essentially planar (the r.m.s. deviations are 0.003) and the greatest deviations from the mean plane are 0.003 5(4) and 0.005 2(4) nm for C19 and C35, respectively. The naphthalene rings are also planar (r.m.s. 0.003) and the greatest deviations from the mean plane are 0.003 6(4) nm for C7 and 0.004 9(3) nm for C26, respectively. The S and N atoms are slightly deviated 0.006 5(1) and 0.008 8(4) nm, and 0.009 6(1) and 0.065 4(4) nm from the maternal naphthalene planes, respectively.

Due to the characteristic conjugated structure of phen and ans ligands, there are not only intramolecular but also intermolecular π-π stacking interactions between adjacent ans and phen ligands. The centroid-centroid distance between the C5-C10 benzene ring (centroid *Cg*1) belonging to the naphthalene ring system and the C39-C43/N4 pyridine ring (*Cg*2) of phen ligand is 0.364 42(19) nm, and the dihedral angle α (between planes *Cg*1 and *Cg*2) and deviation angle β (between the *Cg*1-*Cg*2 vector and the normal to C3-C7/C12 benzene ring) are 7.867 0° and 1.44°, respectively, which indicates that there are significant π-π stacking interactions between phen containing N3/N4 and ans containing S1. At the same time, the planes between intermolecules also show obvious π-π stacking interactions, and the centroid-centroid distances are 0.39044(19) nm for *Cg*2 and *Cg*2^{i} (^{i} 1−*x*, 1−*y*, 1−*z*) and 0.381 03(19) nm for *Cg*3 (N1/C11-C14/C22) and *Cg*4^{ii} (C14-C17/C21-C22; ^{ii} 2−*x*, 1−*y*, 2−*z*), respectively.

Within complex **2**, Pb(Ⅱ)) atom sharing with the same coordination geometry of Cd(Ⅱ) is coordinated by four N atoms of phen ligands, and by two O atoms from monodentate ans ligands. The distances of Pb-N (Table 2), and the mean length of Pb-N is 0.254 5(6) nm, which is in agreement with the distance of Pb-N within $[Pb(phen)(2\text{-ans})_2]_n$ (0.255 3(3) nm; 2-ans is 2-amino-naphthalene-1-sulfonate) [18]. The distance of Pb-O is 0.268 6 (5) nm, which is longer than the length of the equivalent Pb-O in $[Pb(phen)(2\text{-ans})_2]_n$ (0.248 3(3) ~ 0.254 2 (3) nm). The greatest deviations for the mean plane (phen rings) are 0.006 0(9) and 0.008 6(10) nm for C10 and C20, respectively. The greatest deviation of the naphthalene ring is 0.004 0 (9) nm for C28. 0.010 2(7) and 0.003 5(2) nm are the deviations from the naphthalene ring for N1 and S2, respectively.

2.2 UV-Vis spectra

The interactions of $[Cd(phen)_2(ans)_2]\cdot H_2O$ (**1**) and $[Pb(phen)_2(ans)_2]\cdot H_2O$ (**2**) with ctDNA were investigated by means of spectrometric titration and viscosity measurements to evaluate its binding affinities and modes [19]. Electronic absorption spectroscopy was an effective method in examining the interaction with DNA[20]. The absorption spectra of **1** and **2** in the absence and presence of ctDNA at various concentrations were given in Fig.2. Upon increasing concentrations of ctDNA, all the absorption bands of the complexes displayed clear hypochromicities. The absorption bands of **1** at 221.5 and 291 nm exhibited hypochromism of 24% and 21%, respectively, at a ratio of $c_{DNA}/c_{Cd} \approx 3.78$; and the most hypochromism by 33% appeared at 267.5 nm peak with bathochromism of 5 nm ranging from 267.5 nm to 272.5 nm. For **2**, the absorption bands of at

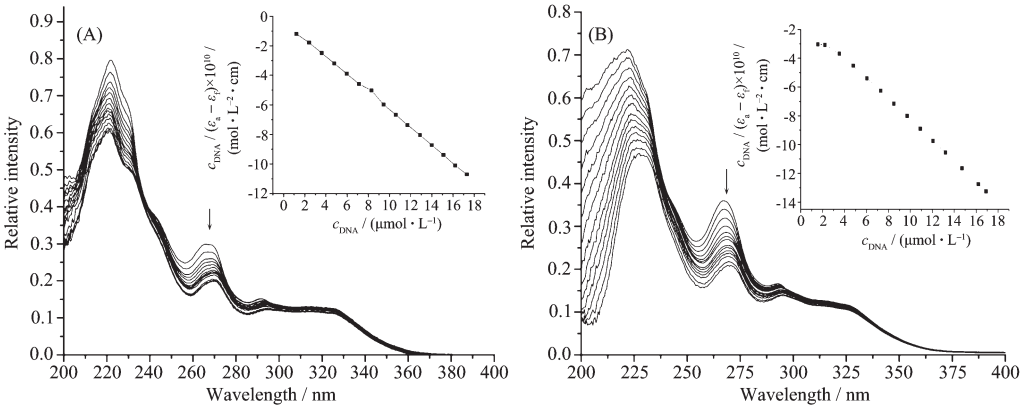

Arrows show the absorbance changes upon increasing ctDNA concentration

Insets: plots of $(\varepsilon_a-\varepsilon_f)/(\varepsilon_b-\varepsilon_f)$ vs c_{DNA} and the linear fit for the titration of the complexes with ctDNA

Fig.2 Absorption spectra of complexes **1** (A) and **2** (B) in 50 mmol·L^{-1} NaCl and 5 mmol·L^{-1} Tris-HCl buffer (pH 7.0) in the presence of increasing amounts of ctDNA (c_M=25 μmol·L^{-1}, c_{DNA}=0~100 μmol·L^{-1})

222, 267 and 292.5 nm exhibited hypochromism of 42.5, 44.45% and 18.5%, and bathochromism of about 6, 4 and 4 nm, respectively, at a ratio of $c_{DNA}/c_{Pb}\approx 3.94$. These results suggest an association of such two complexes with ctDNA.

In order to compare quantitatively the binding strength of the complexes, their intrinsic binding constants with ctDNA were obtained by monitoring the changes in absorbance at 267.5 and 267 nm for **1** and **2**. The following equation was applied[21]:

$$c_{DNA}/(\varepsilon_a-\varepsilon_f)=c_{DNA}/(\varepsilon_b-\varepsilon_f)+1/[K_b(\varepsilon_b-\varepsilon_f)]$$

Where c_{DNA} is the concentration of DNA in base pairs, the apparent absorption coefficients ε_a, ε_f and ε_b correspond to A_{obsd}/c_M, the extinction coefficient for the free complex and the extinction coefficient for the complex in the fully bound form, respectively. The plot $c_{DNA}/(\varepsilon_a-\varepsilon_f)$ vs c_{DNA} gave a slope of $1/(\varepsilon_a-\varepsilon_b)$, and the intercept equals to $1/K_b(\varepsilon_a-\varepsilon_f)$; K_b is the ratio of slope to the intercept. The binding constants K_b of 1.82×10^5 L·mol^{-1} and 4.96×10^4 L·mol^{-1} were obtained for **1** and **2**, respectively. Obviously, the intrinsic constants were smaller than those of the reported Ru(Ⅱ) complexes with semi- or classic intercalation modes into the base pairs of DNA, whereas the degree of hypochromism are much larger than those of Ru(Ⅱ) complexes[22,23]. The reasons for this phenomenon may be that the ratios of $c_{DNA}/c_{Cd}\approx 3.78$ and $c_{DNA}/c_{Pb}\approx 3.94$ are larger than c_{DNA}/c_{Ru} of Ru(Ⅱ) compounds and that the intercalation and electrostatic interaction are coexistence between DNA and **1** or **2**. When the hypochromism and binding constants were calculated, however, the electrostatic interaction was included. The existence of electrostatic interaction would be proved by the luminescence studies later in this paper.

2.3 Luminescence studies

The complexes in aerated buffer solution at room temperature emitted strongly with luminescence peak at 438 nm with the excitations at 251 and 333 nm for **1** and 430 nm with the excitations at 250 and 333 nm for **2**. The changes in emission spectra of the complexes with increasing DNA concentrations are shown in Fig.3. As DNA was successively added into the complex

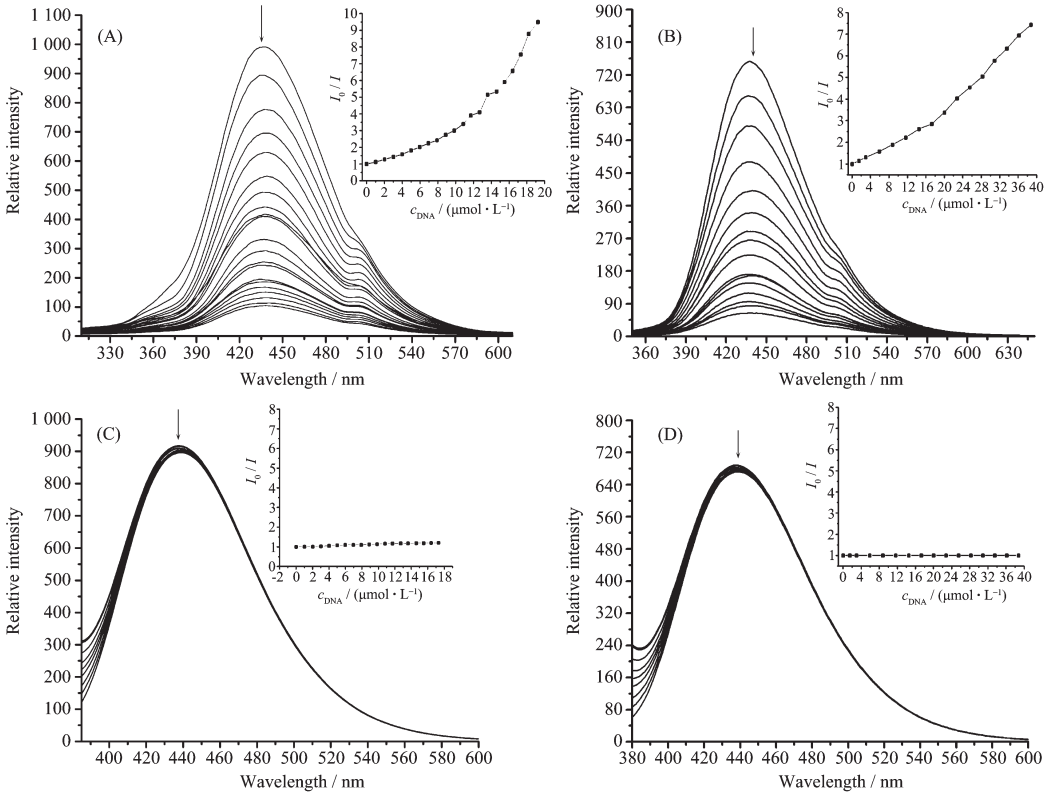

Arrows show the absorbance changes upon increasing ctDNA concentration; Insets: plots of I_0/I vs c_{DNA} and the nonlinear fit for the titration of the complexes with ctDNA

Fig.3　Changes in the emission spectra of complexes **1** and **2** (3.45 μmol·L^{-1}) with increasing concentrations of ctDNA (0~20 μmol·L^{-1} for **1** and 0~40 μmol·L^{-1} for **2**), (A), (B), (C) and (D) are λ_{ex}=251/250 nm and 333 nm for **1** and **2**, respectively

solution, the luminescence intensities of the complexes are hardly changed for the 333 nm excitation. As for the excitation at 251 or 250 nm, however, the emission intensities of both complexes are reduced and have a 10% value of I_0 (c_{DNA}=0 mol·L^{-1}) at $c_{DNA}/c_{Cd}\approx 6.2$ for **1** and 10% at $c_{DNA}/c_{Pb}\approx 10.5$ for **2**. The decrease magnitude is proportional to the complex′s concentration in the buffer, and the quenching magnitude of **1** is larger than that of **2**.

The results of steady-state emission quenching experiments using $[Fe(CN)_6]^{4-}$ as the quencher are shown in Fig.4. In the absence and presence of ctDNA, the emissions of the complexes with excitated wavelength 251 nm for **1** and 250 nm for **2**, were efficiently quenched by $[Fe(CN)_6]^{4-}$. The quenched magnitudes in presence of ctDNA are evidently smaller than those of the absence of ctDNA. However, with or without ctDNA, the intensities of emission changed slightly for the excitated wavelength of 333 nm, which was similar to the results of spectrofluorimetric titration experiments. Obviously, the phenomena are different from the reported compounds bound to ctDNA with intercalation mode[16,17,22,23].

In order to test if the compounds could bind to DNA by intercalation, EB was employed[24,25]. It is well known that EB can intercalate specifically into DNA. Competitive binding of other drugs to DNA and EB will result in displacement of bound EB and a decrease in the fluorescence intensity. However, not only the DNA intercalators but also groove DNA binders can cause the reduction in EB emission intensities[26]. The fluorescence-based competition technique can provide indirect evidence for the DNA-binding mode. Fig.5 presents the emission spectra of DNA-EB system with increasing

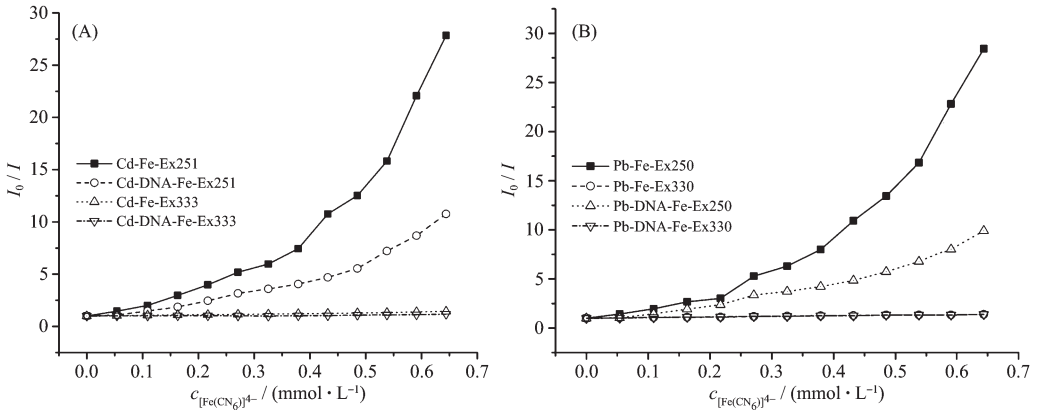

■, ○, △ and ▽ illustrate the relative intensities of emission in the absence of and the presence of ctDNA with λ_{ex}=251/250 nm and 333 nm for **1** and **2**, respectively

Fig.4 Emission quenching of complexes **1** (A) and **2** (B) (20 μmol·L^{-1}) with increasing concentrations of $[Fe(CN)_6]^{4-}$ (0~100 μmol·L^{-1}) in the absence of and the presence of ctDNA (200 μmol·L^{-1})

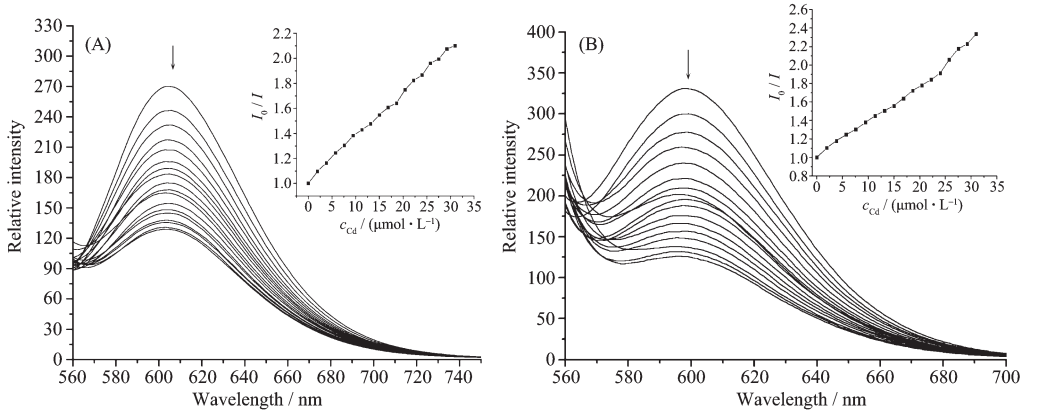

Arrows show the absorbance changes upon increasing the complex concentration; Insets: florescence quenching curves of DNA-bound EB by the complexes; c_{DNA}=50 μmol·L^{-1}, c_{EB}=10 μmol·L^{-1} and λ_{ex}=535 nm

Fig.5 Emission spectra of EB bound to ctDNA in the presence of complexes **1** (A) (0~35 μmol·L^{-1}) and **2** (B) (0~45 μmol·L^{-1})

amounts of **1** and **2**. It is clear that the fluorescence intensity of DNA-EB system decreases upon the addition of the complexes. The results imply that the complexes may bind to ctDNA via intercalation mode, because they can not be bound to DNA in the groove sites. According to linear Stern-Volmer equation, the K_q values for **1** and **2** are 3.5×10^4 and 1.4×10^4 L·mol^{-1}, respectively. This order is well consistent with the results of spectrofluorimetric titration.

Besides the results of the competitive binding experiments, the other fluorescent phenomena are different from those observed for Ru(Ⅱ) complexes binding to DNA in semi- or classical intercalation modes. The reasonable explanations may be followings: first, the complexes are constructed by 1,10-phenanthroline and 4-aminonaphthalene-1-sulfonate, which both ligands exhibit good luminescence properties. In buffer solution, the excitations and emissions are 245 and 435 nm for 4-aminonaphthalene-1-sulfonate, 302 and 384 nm for 1,10-phenanthroline, respectively. Due to the coordination to metal atom, the excitations are red-shift to 250/251 and 333 nm in the complexes, which is different from the electrolyte complex [Cd(phen)$_2$](NO$_3$)$_2$ emitted luminescence peak at 363 nm with excitation 293 nm[27]. Second, the molecular structures of the complexes are different from those of Ru(Ⅱ) complexes, despite of having the same distorted octahedral coordination geometries, as shown in Fig.1. No doubt, the complexes have larger steric hindrance to the binding ability to ctDNA than the reported Ru(Ⅱ) complexes. On the other hand, the amino H atoms laying the other end of naphthalene ring can form hydrogen bonds with O atoms from the deoxyribose-phosphate backbone. Third, as a common fluorescence quencher $[Fe(CN)_6]^{4-}$ can reduce the emission intensity of 4-aminonaphthalene-1-sulfonate, but can not quench 1,10-phenanthroline in buffer. Thus, the intercalator was 1,10-phenanthroline and hydrogen bond was simultaneously formed by amino H and O belonging to the phosphate, and the interaction was smaller than the reported Ru(Ⅱ) complexes demonstrated by the binding and quenching constants. The combined interactions cause the remarkable decrease of luminescence peaks for 251/250 nm excitation and negligible change for the 333 nm excitation. Based on the same reasoning, it is acceptable that the results of the steady-state emission quenching experiment are similar to those of spectrofluorimetric titration.

Taking changes about conformation of DNA and electrostatic potential into account, the cationic molecule is usually more favorable than the uncharged compound associated with DNA [28,29]. The DNA binding constant for EB is 2.6×10^5 L·mol^{-1} (I=0.1 mol·L^{-1})[24,30], hence the much larger ratios of $c_{Cd}/c_{EB}\approx2.7$ and $c_{Pb}/c_{EB}\approx3.4$ were acceptable. Furthermore, the quenching constants K_q 3.5×10^4 L·mol^{-1} and 1.4×10^4 L·mol^{-1} of 1 and 2 are greatly smaller than those of Ru(Ⅱ) complexes, which is also in agreement with the results of electronic absorption titration with the binding constants K_b (1.82×10^5 L·mol^{-1} and 4.96×10^4 L·mol^{-1}) through electrostatic absorption titration.

2.4 Viscosity studies

Optical photophysical probes provide necessary, but not sufficient, evidence to support the binding mode of the complex[12]. To clarify the nature of the interaction between the complexes and DNA further, viscosity measurements were carried out and the results were presented in Fig.6. Intercalation is expected to lengthen the DNA helix as the base pairs are pushed apart to accommodate the bound ligand, leading to an increase in the DNA viscosity. In contrast, a partial, non-classical intercalation of ligand could bend (or kink) the DNA helix, reduces its effective length and, concomitantly, its viscosity [12]. On the other hand, for $[Ru(bipy)_3]^{2+}$, which has been well known to bind with DNA by the electrostatic mode, there is no effect on the relative viscosity of the DNA solution[31]. In our case, as

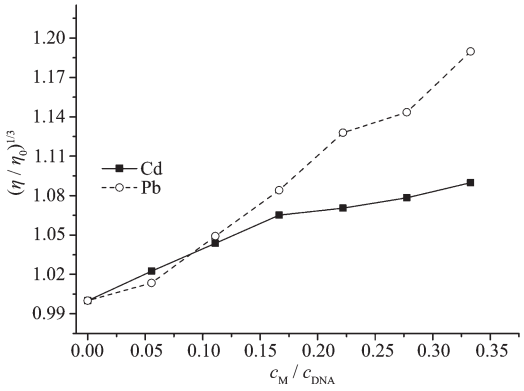

Fig.6　Effect of increasing amounts of complexes **1** (■) and **2** (○) on the relative viscosity of ctDNA (0.45 mmol·L^{-1}) at 28±0.1 ℃

shown in Fig.6, with an increasing amount of the complexes, the relative viscosities of DAN were slowly aggrandized, which was similar to and smaller than the effects of most reported complexes with intercalation to DNA, such as $[Ru(phen)_3]^{2+}$, $[Ru(phen)_2dppz]^{2+}$ and $[Ru(bipy)_2dppz]^{2+}$ as well [22,23,31]. And these results are well consistent with the results absorption and fluorescence experiments.

3 Conclusions

In summary, two organosulfonate complexes $[Cd(phen)_2(ans)_2]\cdot H_2O$ and $[Pb(phen)_2(ans)_2]\cdot H_2O$ had been synthesized and characterized. The Cd^{2+} and Pb^{2+} having the same coordination geometries are respectively coordinated by four N atoms from two phen ligands and by two O atoms from ans ligands, showing a distorted octahedral environment. The experimental results of UV-Visible spectra, luminescence studies and viscosity measurements reveal that the complexes bind to DNA by means of intercalation and electrostatic interaction binding models. DNA-binding affinity of **1** is higher than that of **2**. As the neutral complexes, their abilities to bind to ctDNA are weaker than those of the cationic complexes. Based on these results, the cationic complexes containing aromatic sulfonate are in progress.

References:

[1] Demeunynck M, Bailly C, Wilson W D. *DNA and RNA Binders*. Weinheim: Wiley-VCH, **2000**.

[2] Marcel Ecker. *Metal Ions in Biological Systems*, New York, **1996**,**33**:177~252

[3] Erkkilia K E, Odom D T, Barton J K. *Chem. Rev.*, **1999**,**99**: 2777~2796

[4] Balzani V, Juris A, Venturi M, et al. *Chem. Rev.*, **1996**,**96**:759 ~834

[5] Xu H, Zheng K Z, Chen Y, et al. *Dalton Trans.*, **2003**:2260~ 2268

[6] Xiong Y, Ji L N. *Coord. Chem. Rev.*, **1999**,**185~186**:711~733

[7] Liu J G, Zhang Q L, Shi X F, et al. *Inorg. Chem.*, **2001**,**40**: 5045~5050

[8] Zou X H, Ye B H, Li H, et al. *J. Chem. Soc., Dalton Trans.*, **1999**:1423~1428

[9] Lerman L S. *Proc. Natl. Acad. Sci., USA*, **1963**,**49**:94~102

[10]Geary W J. *Coord. Chem. Rev.*, **1971**,**7**:81~122

[11]Reichmann M E, Rice S A, Thomas C A, et al. *J. Am. Chem. Soc.*, **1954**,**76**:3047~3053

[12]Satyanarayana S, Daborusak J C, Chaires J B. *Biochem.*, **1993**,**32**:2573~2584

[13]Sheldrick G M. *SADABS*: *Program for Empirical Absorption Correction of Area Detector Data*, University of Göttingen, Germany, 1996.

[14]Sheldrick G M. *SHELXL*97, *Program for Crystal Structure Refinement*, University of Göttingen, Germany, **1997**.

[15]Spek A L. *Acta Crys. Sect.*, **1990**,**A46**:C34

[16]Yam V W W, Pui Y L, Cheung K K. *New J. Chem.*, **1999**,**23**: 1163~1169

[17]Chen C H, Cai J W, Liao C Z, et al. *Inorg. Chem.*, **2002**,**41**: 4967~4974

[18]Cui Z N, Guo J H, Yang E C. *Chin. J. Struct. Chem.*, **2007**,**6**: 717~720

[19]Fox K R. *Drug-DNA Interaction Protocols*. Totowa, N J: Humana Press, **1997**.

[20]Barton J K, Danishefsky A T, Golderg J M. *J. Am. Chem. Soc.*, **1984**,**106**:2172~2176

[21]Wolfe A, Shimer G H, Meehan T. *Biochem.*, **1987**,**26**:6392~ 6396

[22]Pyle A M, Rehmann J P, Meshoyrer R, et al. *J. Am. Chem. Soc.*, **1989**,**111**:3051~3058

[23]Haq I H, Lincoln P, Suh D, et al. *J. Am. Chem. Soc.*, **1995**, **117**:4788~4796

[24]Boger D L, Fink B E, Brunette S R, et al. *J. Am. Chem. Soc.*, **2001**,**123**:5878~5891

[25]Horton D A, Bourne G T, Smythe M L. *Chem. Rev.*, **2003**, **103**:893~930

[26]Kelly J M, Tossi A B, Meconnell D J, et al. *Nucleic Acids Res.*, **1985**,**13**:6017~6034

[27]YANG Zhou-Sheng(杨周生), YU Jun-Sheng(于俊生), CHEN Hong-Yuan(陈洪渊). *Chinese J. Inorg. Chem.*(*Wuji Huaxue Xuebao*), **2002**,**18**(4):373~377

[28]Herzyk P, Neidle S, Goodfellow J M. *J. Biomol. Struct. Dyn. A*, **1992**,**10**:97~140

[29]Friedman R A, Manning G S. *Biopolymers*, **1984**,**23**:2671~ 2714

[30]Fang Y Y, Ray B D, Caussen C A, et al. *J. Am. Chem. Soc.*, **2004**,**126**:5403~5412

[31]Kumar C V, Barton J K, Turro M J. *J. Am. Chem. Soc.*, **1985**, **107**:5518~5523